BJR https://doi.org/10.1259/bjr.20160849

Received: 03 November 2016 | Revised: 11 December 2017 | Accepted: 19 April 2018



Cite this article as:
Zhong R, Song Y, Yan Y, Wang X, Li S, Zhou J, et al. Analysis of which local set-up errors can be covered by a 5-mm margin for cone beam CT-guided radiotherapy for nasopharyngeal carcinoma. *Br J Radiol* 2018; **91**: 20160849.

FULL PAPER

# Analysis of which local set-up errors can be covered by a 5-mm margin for cone beam CT-guided radiotherapy for nasopharyngeal carcinoma

**[1]RENMING ZHONG, [1]YING SONG, [2]YUYING YAN, [1]XUETAO WANG, [1]SHUAI LI, [1]JIDAN ZHOU, [1]XIAOYU LI and [1]SEN BAI**

[1]Division of Radiation Physics, State Key Laboratory of Biotherapy and Cancer Center, West China Hospital, Sichuan University, Chengdu, China
[2]Oncology Department of Sichuan Academy of Medical Science & Sichuan Provincial People's Hospital, Chengdu, China

Address correspondence to: Mr Sen Bai
E-mail: *1458948580@qq.com; baisen@scu.edu.cn*

The authors Renming Zhong, Ying Song and Yuying Yan contributed equally to the work.

**Objective:** To analyse which local set-up errors can be covered by a 5-mm margin for cone beam computed tomography (CBCT)-guided radiotherapy in nasopharyngeal carcinoma (NPC).
**Methods:** 11 regions of interest (ROIs) were registered for 24 NPC patients, with a total of 323 CBCT scans. According to the registration results, clinical target volume–planning target volume (CTV–PTV)/organs at risk-planning risk volume (OAR-PRV) margin analysis; Pearson correlation analysis; Bland–Altman plots; and a receiver operating characteristic (ROC) analysis were used to investigate which local set-up errors of substructure can be represented by the $PTV_{ROI}$.
**Results:** The clinical target volume-PTV/OAR-planning risk volume margins were less than 5 mm for $C1_{ROI}$-$C4_{ROI}$, mandible ($M_{ROI}$), and sphenoid sinus ($S_{ROI}$) with respect to $PTV_{ROI}$. $C1_{ROI}$-$C4_{ROI}$, $M_{ROI}$, and $S_{ROI}$ exhibited significant correlations and consistencies in the mediolateral, superior–inferior, and anteroposterior (AP) directions and significant receiver operating characteristic analysis results in the anteroposterior direction.
**Conclusion:** Only the upper local set-up error of $C1_{ROI}$-$C4_{ROI}$, $M_{ROI}$, and $S_{ROI}$ can be covered by a 5-mm margin for CBCT-guided NPC radiotherapy with a large ROI. Using these ROIs as an integral reference ROI is better than individual bony landmark.
**Advances in knowledge:** This report is helpful to CBCT registration for NPC radiotherapy in clinical practice.

## BACKGROUND AND PURPOSE

With large irradiation volumes and the involvement of multiple organs at risk (OAR), a high level of set-up position repeatability is required in radiotherapy for nasopharyngeal carcinoma (NPC) patients. Recently, a number of radiotherapy techniques have been reported, such as intensity modulated radiotherapy and volume modulated arc therapy, which provides uniform dose distributions, steeper dose fall-offs, and reduced irradiation volumes. Therefore, image-guided radiotherapy is considered to be an essential tool in ensuring the safe clinical application of these techniques.

For the outstanding performance, cone beam computed tomography (CBCT) has been widely applied in position verification. In addition, the set-up error can be corrected online according to the registration results. In many institutions, the planning target volume (PTV) is customarily set as region of interest (ROI) for automatic bone registration.[1,2] Meanwhile, the 5-mm clinical target volume, CTV–PTV and OAR-planning risk volume (PRV) margins are popularly used for NPC radiotherapy.[1,3] However, there is the potential for radiation injury from OARs or treatment failure from CTVs due to the local set-up errors.[1–5] The purpose of this article was to analyse local set-up errors for substructures, and to investigate which local set-up errors can be covered by a 5mm margin for CBCT-guided NPC radiotherapy.

## METHODS AND MATERIALS

24 NPC patients treated in West China Hospital from July 2012 to April 2014 were included in this study. The patients

included 15 (62.5%) females and 9 (37.5%) males ranging in age from 18 to 65 years. All patients had poorly differentiated squamous cell carcinomas confirmed by pharyngorhinoscopy, and the tumour stages ranged from I to IV according to the American Joint Committee on Cancer cancer staging manual. All patients were immobilised with a thermoplastic mask and a standard C-type headrest. The planning CT scans were performed in the same treatment positions from the cranium to the sternum with a slice distance of 3 mm. Intensity modulated radiotherapy or volumetric modulated arc therapy planning with 5 mm CTV/OAR expanding margins (brain stem, spinal cord) were generated in the Pinnacle planning system (Pinnacle 9.2, Philips Medical Systems, Fitchburg, WI). In some cases, the margins were intentionally trimmed to avoid the brain stem or the optic chiasm. The total doses were 73.92 Gy (2.24 Gy × 33 fractions, 11 patients) and 69.96 Gy (2.12 Gy × 33 fractions, 13 patients) to the primary tumour, 60 Gy to the high-risk involved tissues and the suspicious node drainage area, and 56 Gy to the low-risk regions (CTV2). The maximum length of the craniocaudal treatment field was 25 cm.

Each CBCT scan was performed with an Elekta Synergy XVI 4.5 imaging system (Synergy, Elekta, Crawley, UK). For each patient, a CBCT scan for the first three treatment fractions was essential. Then, at least one CBCT scan was obtained per week in subsequent fractions. The median number of CBCT scans per patient was 14 (range 7–33). One patient had only seven CBCT scans due to a small set-up error for the first three fractions and a score of 3 of Eastern Cooperative Oncology Group performance state in subsequent fractions. During the CBCT scanning, the gantry rotated over 200° at 3.18° $s^{-1}$, and a total of 361 projections were acquired with a spatial resolution of 0.1 cm per pixel. To improve the image quality and reduce the scanning area, the collimator cassette S20 was used and the field of view was 26 cm.

In clinical practice, automatic bone registration with $PTV_{ROI}$ was performed between the CBCT and planning CT (Elekta Synergy XVI 4.5 imaging system, Synergy, Elekta, Crawley, UK). The online correction protocol was 2 mm in any translational direction. To evaluate local set-up errors, individual bony landmark was set as ROI and registrated between the CBCT and planning CT. These bony landmarks included the cervical vertebrae C1-C7 (*i.e.* $C1_{ROI}$, $C2_{ROI}$, $C3_{ROI}$, $C4_{ROI}$, $C5_{ROI}$, $C6_{ROI}$, and $C7_{ROI}$), mandible ($M_{ROI}$), larynx ($L_{ROI}$), and sphenoid sinus ($S_{ROI}$) (Figure 1). The region below the first thoracic vertebra ($T_1$) was not defined as ROI due to the poor image quality in CBCT. First, the automatic bony registration was performed to achieve a fast and coarse matching. Then, manual fine adjustments were followed by visual inspection. These two steps were performed carefully to guarantee the registration accuracy of each individual ROI for our offline registration protocol. To verify the validation of our registration method, $S_{ROI}$ registration results of 10 patients performed by two therapists were compared. The registration result was reproducible (with a standard deviation <1 mm). According to the equations given on p. 37 of the British Institute of Radiology report on geometric uncertainty, the group mean

Figure 1. 10 three-dimensional rectangular-shaped ROIs around individual bones and large ROI ($PTV_{ROI}$) were defined in sagittal view. Solid line represents large ROI ($PTV_{ROI}$), dotted line represents individual bones [*i.e.* $C1_{ROI}$, $C2_{ROI}$, $C3_{ROI}$, $C4_{ROI}$, $C5_{ROI}$, $C6_{ROI}$ and $C7_{ROI}$, mandible ($M_{ROI}$), larynx ($L_{ROI}$), and sphenoid sinus ($S_{ROI}$)]. PTV, planning target volume; ROIs, regions of interest.

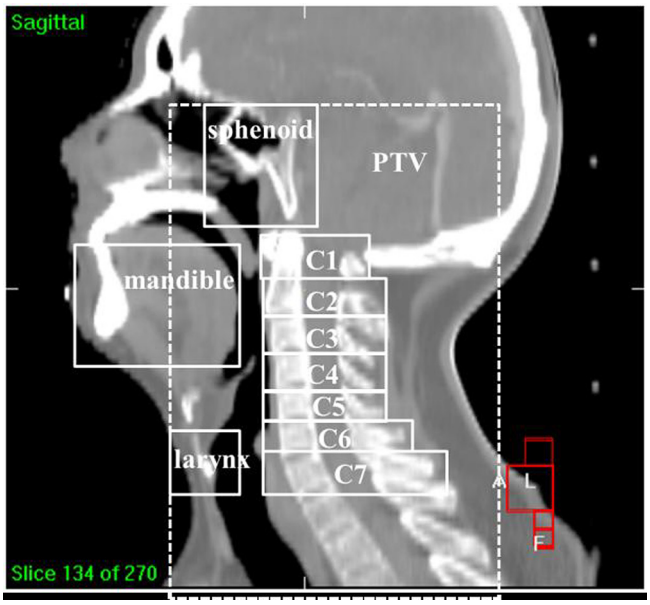


error (M), systematic (Σ) error, and random error (σ) were computed along three translational axes [*i.e.* the mediolateral (ML), superior–inferior (SI), and anteroposterior (AP) directions]; and the rotational axes [*i.e.* the *x* (pitch), *y* (roll), and *z* (yaw)].[6]

The CTV–PTV/OAR-PRV margins were generated based on the van Herk equation (2.5Σ +0.7σ).[6] To investigate which local set-up errors could be covered by a 5-mm margin, the differences in the translational errors and rotational errors between $PTV_{ROI}$ and other ROIs were calculated. Then, the corresponding CTV–PTV/OAR-PRV margins were compared. To determine which ROI pairs have significant correlations, the Pearson correlation coefficients of registration results for different ROIs were transferred to a colour plot.[1] We also assessed the consistency of local set-up errors for these ROIs using Bland–Altman analysis.[7] According to our clinical routine, the online correction protocol was set as 2 mm of translational error in any direction. To investigate the difference of online correction between $PTV_{ROI}$ and other ROIs, the registration results of other ROIs were divided into two groups with a threshold of 2 mm. Then, the analysis of receiver operating characteristic (ROC) curves was performed using grouping of $PTV_{ROI}$ as the gold standard.[8]

## RESULTS

Among all the ROIs, the registration results of $PTV_{ROI}$ exhibited lower translational errors (Table 1) than all the other ROIs and lower rotational errors than the majority of the other ROIs (Supplementary Table 1). The corresponding margins were

Table 1. Translational errors for each ROI and the corresponding margins (mm)

| ROI | | M | Σ | σ | Margin | ROI | | M | Σ | σ | Margin |
|---|---|---|---|---|---|---|---|---|---|---|---|
| $PTV_{ROI}$ | ML | 0.2 | 1.2 | 1.2 | 3.9 | $C6_{ROI}$ | ML | 0.1 | 1.5 | 1.6 | 5.0 |
| | SI | 0.5 | 1.5 | 1.3 | 4.5 | | SI | 0.9 | 1.9 | 1.5 | 5.8 |
| | AP | 0.7 | 1.0 | 1.0 | 3.2 | | AP | 0.9 | 3.0 | 2.3 | 9.0 |
| $C1_{ROI}$ | ML | 0.2 | 1.5 | 1.4 | 4.7 | $C7_{ROI}$ | ML | 0.0 | 1.5 | 1.6 | 4.9 |
| | SI | 0.7 | 1.9 | 1.4 | 5.7 | | SI | 0.8 | 1.9 | 1.5 | 5.9 |
| | AP | 0.2 | 1.5 | 1.5 | 4.9 | | AP | 1.1 | 3.0 | 2.4 | 9.1 |
| $C2_{ROI}$ | ML | 0.2 | 1.4 | 1.5 | 4.6 | $S_{ROI}$ | ML | 0.2 | 1.8 | 1.7 | 5.7 |
| | SI | 0.7 | 1.9 | 1.5 | 5.8 | | SI | 0.4 | 1.7 | 1.3 | 5.2 |
| | AP | 0.3 | 1.5 | 1.4 | 4.7 | | AP | −0.7 | 1.8 | 1.8 | 5.8 |
| $C3_{ROI}$ | ML | 0.1 | 1.3 | 1.4 | 4.3 | $M_{ROI}$ | ML | 0.4 | 1.7 | 1.7 | 5.4 |
| | SI | 0.7 | 1.9 | 1.4 | 5.8 | | SI | 1.0 | 1.8 | 1.6 | 5.6 |
| | AP | 0.5 | 1.6 | 1.4 | 5.0 | | AP | 0.2 | 1.4 | 1.6 | 4.7 |
| $C4_{ROI}$ | ML | 0.0 | 1.4 | 1.6 | 4.6 | $L_{ROI}$ | ML | 0.9 | 1.7 | 1.6 | 5.4 |
| | SI | 0.8 | 1.9 | 1.5 | 5.8 | | SI | 0.0 | 2.7 | 2.4 | 8.3 |
| | AP | 0.7 | 2.0 | 1.6 | 6.1 | | AP | 0.9 | 2.2 | 1.9 | 6.8 |
| $C5_{ROI}$ | ML | 0.1 | 1.4 | 1.6 | 4.6 | | | | | | |
| | SI | 0.9 | 1.8 | 1.6 | 5.7 | | | | | | |
| | AP | 0.9 | 2.7 | 2.1 | 8.3 | | | | | | |

AP, anteroposterior; ML, mediolateral; ROI, region of interest; SI, superior–inferior.
The group mean error (M), systematic (Σ) and random errors (σ) were calculated according the equations given on page 37 of the BIR report on geometric uncertainty. Margin = 2.5Σ +0.7σ.

3.7 mm (ML), 4.5 mm (SI), and 3.3 mm (AP). However, the margins in the SI direction exceeded 5 mm for $C1_{ROI}$, $C2_{ROI}$, $C3_{ROI}$, and $C4_{ROI}$. Using $PTV_{ROI}$ as a reference (Table 2), the margins of $C5_{ROI}$, $C6_{ROI}$, and $C7_{ROI}$ in the AP direction were 7.2 mm, 8.3 mm, and 8.1 mm, respectively. Regarding rotation (Supplementary Table 2), $S_{ROI}$ and $M_{ROI}$ exhibited the smallest

Table 2. The differences and corresponding margins in the translational errors between the $PTV_{ROI}$ and the other ROIs (mm)

| ROI | | M | Σ | σ | Margin | ROI | | M | Σ | σ | Margin |
|---|---|---|---|---|---|---|---|---|---|---|---|
| $S_{ROI}$ | ML | 0.1 | 1.1 | 0.7 | 3.2 | $C5_{ROI}$ | ML | 0.1 | 1.1 | 0.7 | 3.2 |
| | SI | −0.1 | 0.7 | 0.5 | 2.0 | | SI | −0.4 | 1.0 | 0.7 | 2.9 |
| | AP | 1.4 | 1.3 | 1.3 | 4.3 | | AP | −0.2 | 1.7 | 2.4 | 6.0 |
| $C1_{ROI}$ | ML | 0 | 0.8 | 0.5 | 2.4 | $C6_{ROI}$ | ML | 0.1 | 1.1 | 0.9 | 3.4 |
| | SI | −0.3 | 0.7 | 0.8 | 2.2 | | SI | −0.4 | 0.9 | 0.9 | 2.8 |
| | AP | 0.5 | 1.0 | 1.0 | 3.1 | | AP | −0.2 | 2.0 | 2.7 | 6.8 |
| $C2_{ROI}$ | ML | 0 | 0.9 | 0.6 | 2.6 | $C7_{ROI}$ | ML | 0.1 | 1.2 | 0.9 | 3.8 |
| | SI | −0.2 | 0.7 | 0.8 | 2.3 | | SI | −0.4 | 0.9 | 0.9 | 2.9 |
| | AP | 0.4 | 0.9 | 0.9 | 2.9 | | AP | −0.3 | 2.1 | 2.5 | 6.9 |
| $C3_{ROI}$ | ML | 0 | 0.8 | 0.5 | 2.5 | $M_{ROI}$ | ML | −0.1 | 0.9 | 0.6 | 2.8 |
| | SI | −0.2 | 0.7 | 0.8 | 2.3 | | SI | −0.7 | 1.0 | 0.9 | 3.1 |
| | AP | 0.2 | 1.0 | 1.1 | 3.1 | | AP | 0.6 | 1.0 | 0.9 | 3.1 |
| $C4_{ROI}$ | ML | 0.1 | 1.0 | 0.7 | 3.1 | $L_{ROI}$ | ML | −0.6 | 1.5 | 0.7 | 4.2 |
| | SI | −0.3 | 0.8 | 0.7 | 2.5 | | SI | 0.3 | 2.2 | 3.3 | 7.8 |
| | AP | 0 | 1.2 | 1.5 | 4.1 | | AP | −0.1 | 1.7 | 2.1 | 5.8 |

AP, anteroposterior; ML, mediolateral; PTV,planning target volume; ROI, region of interest; SI, superior–inferior.
The group mean error (M), systematic (Σ) and random errors (σ) were calculated according the equations given on p. 37 of the BIR report on geometric uncertainty. Margin = 2.5Σ +0.7σ.

Figure 2. Colour plots of the Pearson correlation coefficients for the translational errors and rotational errors between each ROI. The highlighted area indicates the higher correlation coefficients, and the dark colour indicates the lower correlation coefficients. PTV, planning target volume; ROI, region of interest.

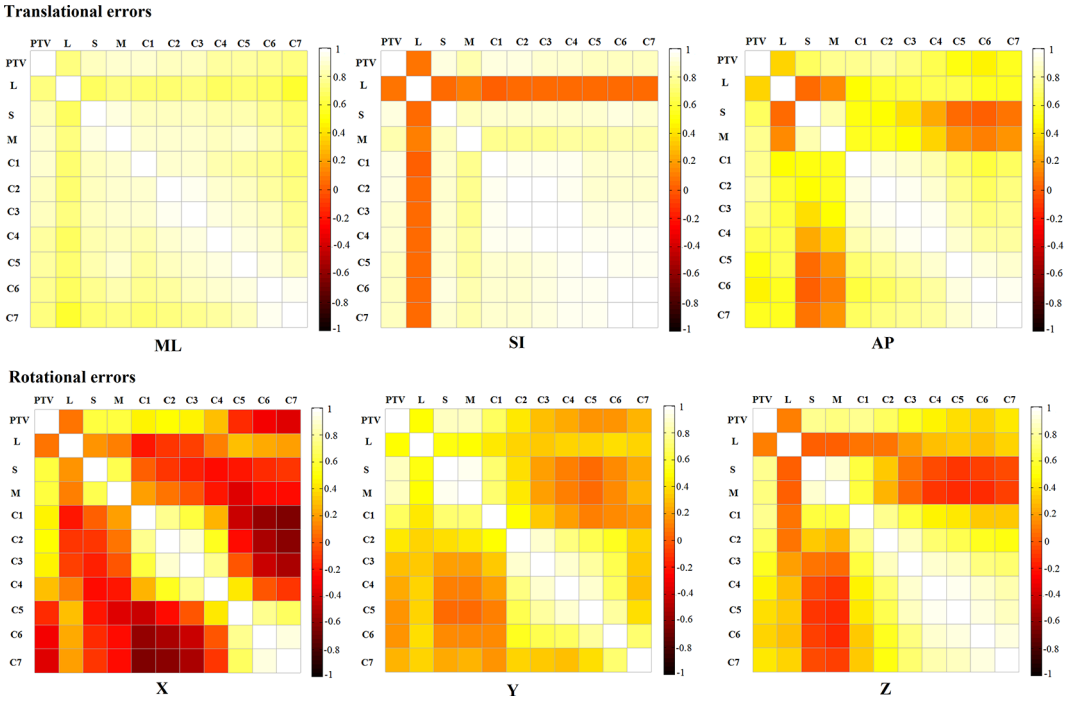


differences compared to $PTV_{ROI}$, with systematic and random local set-up errors of less than 1°.

The colour plots showed that the translational errors exhibited better correlation coefficients than the rotational errors among these ROIs (Figure 2). There were high correlation coefficients (ranged from 0.588 to 0.945) in ML and SI directions among these ROIs, except for $L_{ROI}$ in SI direction (ranged from 0.007 to 0.118). The $C1_{ROI}$-$C7_{ROI}$ regions exhibited better correlations in the SI direction, especially in the $C1_{ROI}$-$C4_{ROI}$ regions (ranged 0.945–0.73). The lower correlation coefficients were found between the $S_{ROI}$, $M_{ROI}$ and the $C4_{ROI}$-$C7_{ROI}$ regions (ranged 0.071–0.352) in AP direction. However, there were negative correlations between the $C1_{ROI}$-$C4_{ROI}$ regions and the $C5_{ROI}$-$C7_{ROI}$ regions (ranged from −0.026 to −0.635) in pitch. The lower or negative correlations were found between the $S_{ROI}$, $M_{ROI}$ and the $C1_{ROI}$-$C7_{ROI}$ regions (ranged from −0.249 to 0.213) in pitch. As to the roll direction, there were lower correlation coefficients between the $S_{ROI}$, $M_{ROI}$ and the $C3_{ROI}$ regions and the $C3_{ROI}$-$C7_{ROI}$ regions (ranged from 0.04 to 0.325).The negative correlations were found again between the $S_{ROI}$, $M_{ROI}$ and the $C4_{ROI}$-$C7_{ROI}$ regions (ranged from −0.09 to −0.155) for rotational errors in yaw direction. In terms of same axis for all ROIs, there were higher correlation coefficients between the $PTV_{ROI}$ and the $C1_{ROI}$-$C4_{ROI}$ regions.

The Bland–Altman analysis demonstrated significant registration consistency between the $PTV_{ROI}$ and $C1_{ROI}$-$C4_{ROI}$, $S_{ROI}$, and $M_{ROI}$. Figure 3 showed a strong registration consistency between $PTV_{ROI}$ and $S_{ROI}$. As expected, the ROIs below the C5 level (*i.e.* $C5_{ROI}$, $C6_{ROI}$, $C7_{ROI}$, and $L_{ROI}$) show relatively poor registration agreement with the $PTV_{ROI}$.

The ROC analyses show that all ROIs in the SI direction and $C1_{ROI}$-$C4_{ROI}$, $S_{ROI}$, and $M_{ROI}$ in the AP direction had discrimination power according to grouping of $PTV_{ROI}$ (Table 3). No significant ROC analysis results were observed between the grouping of $PTV_{ROI}$ and other ROIs in the ML direction.

## DISCUSSION

Similar to other studies, we found considerable set-up errors among multiple fractions in head and neck cancer radiotherapy despite the use of immobilisation devices.[2,4,9–11] The CTV–PTV margins largely depend on the immobilisation devices, the radiation method, and the frequency of verification imaging. Some studies have shown that a 5-mm CTV–PTV margin is required in head and neck cancer radiotherapy.[1,12,13] In some cases, a 3-mm CTV–PTV margin has been used due to the proximity with or even the overlapping of a large portion of a critical structure with the tumour.[14] With no image guidance, 40.8% of fractions would have been more than5 mm off-target.[15] Thus, image-guided radiotherapy is helpful for head and neck radiotherapy.[10,14,16]

However, usually, the local set-up errors were neglected in the previously mentioned margin protocols. The margin protocol depends on a measured system and random errors. The image-guided radiotherapy registration strategy (*e.g.* selecting the appropriate ROI) determined the measured system and random error, and the couch correction ultimately influences the resulting dose distributions.[5,17,18] Some authors reported that the $C1_{ROI}$, $C2_{ROI}$, and $C3_{ROI}$ region group were used as a reference landmark to evaluate the local set-up errors.[1,5] Consistent with other reports,[2,3] our results show that these errors were primarily focused in the SI direction and corresponding margins exceeded 5 mm using the $C1_{ROI}$, $C2_{ROI}$, $C3_{ROI}$, and

Figure 3. Bland–Altman error analysis for the $PTV_{ROI}$ *vs* $S_{ROI}$ registration results in translational directions ML, SI, and AP and rotational axes *x*, *y*, *z*. The abscissa indicates the mean of registration errors between $PTV_{ROI}$ and $S_{ROI}$, and the ordinate indicates the difference of registration errors between $PTV_{ROI}$ and $S_{ROI}$ ($PTV_{ROI}$-$S_{ROI}$). Solid black lines are the 95% confidence interval. Dashed black line is the mean of the difference. The number of points that exceeded the 95% confidence interval were less than 16 (5% of the total registration number 323), which indicated that $PTV_{ROI}$ and $S_{ROI}$ have strong registration consistency. AP, anteroposterior; ML, mediolateral; PTV, planning target volume; ROI, region of interest; SI, superior–inferior.

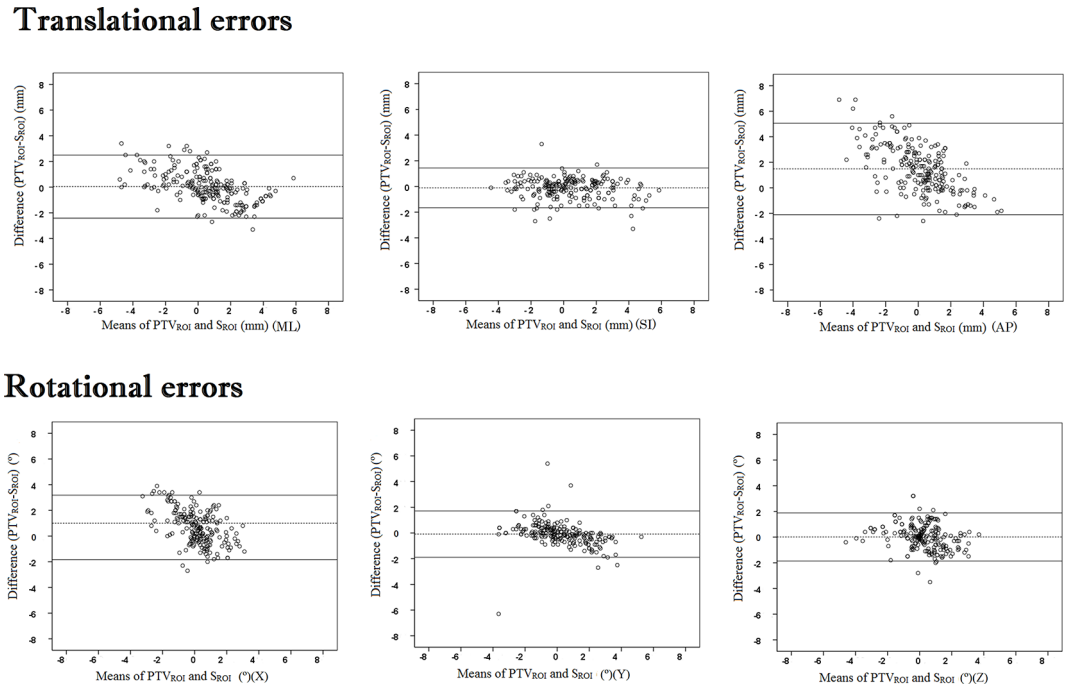


$C4_{ROI}$ alone as reference landmark. Meanwhile, Djordjevic et al recommended that the image registration should be based on a small region according to GTV and OARs.[19] In our study, the GTVs of NPC are primarily located around the sphenoid sinus, and such tumours were in close proximity to the brain stem or optical nerves. Thus, registrations that focused on the sphenoid sinus ($S_{ROI}$) were superior to the $C1_{ROI}$, $C2_{ROI}$, and $C3_{ROI}$ region group registration in terms of the OAR sparing of the nearby tissues because smaller margins are required in this area.[2] Thirdly, there was lower or negative relationship between the group of $C1_{ROI}$-$C3_{ROI}$ and the group of $M_{ROI}$, $S_{ROI}$ in pitch. The negative relation was found again between the group of $C1_{ROI}$-$C3_{ROI}$ and the group of $C5\_C7_{ROI}$ in the same axes (Figure 2). Therefore, in our opinion, using the $C1_{ROI}$, $C2_{ROI}$, and $C3_{ROI}$ as reference landmark for registration was unsuitable in nasopharyngeal cancer radiotherapy.

In routine practice, using $PTV_{ROI}$ as a reference has verified four significant statistical results, as follows: (1) it was easy to find that the $PTV_{ROI}$ registration results exhibited minimal differences from the region of $C1_{ROI}$-$C4_{ROI}$ and $M_{ROI}$, of which the CTV–PTV margins were all within the 5 mm limit. However, the results were different for the $C5_{ROI}$-$C7_{ROI}$ regions, which exhibited more than 7 mm OAR-PRV margins in the AP direction. (2) The correlation analysis vividly demonstrated that there was a significant correlation between $PTV_{ROI}$, $C1_{ROI}$-$C4_{ROI}$, $M_{ROI}$, and $S_{RO}$I. (3) The Bland–Altman plots indicated high registration consistency between $PTV_{ROI}$, $C1_{ROI}$-$C4_{ROI}$, $M_{ROI}$, and $S_{ROI}$, respectively, and the low levels for the ROI group $C5_{ROI}$-$C7_{ROI}$ and $L_{ROI}$. (4) Similar results were observed in the ROC analysis in the AP direction. ROC analysis showed no significant results for any of the ROIs in the ML direction. However, the local set-up errors of substructures in the ML direction were smaller than those in the SI and AP directions, which required margins of less than 5 mm. According to these findings, we can conclude that the local set-up error of $C1_{ROI}$-$C4_{ROI}$, $M_{ROI}$, and $S_{ROI}$ can be represented by $PTV_{ROI}$ in CBCT-guided NPC radiotherapy with a 5-mm margin scheme. In other words, using these ROIs as an integral reference ROI was better than individual bony landmark.

In this study, the CTV–PTV/OAR-PRV margins calculated based on $PTV_{ROI}$ were less than 5 mm in three axes. However, the registrations based on the other ROIs all yielded PTV margins greater than 5 mm. Djordjevic M et al reported that the CTV–PTV margins for the subregions ranged from 4.5 to 9.3 mm with no image guidance and from 2.3 to 6.8 mm with daily image guidance.[19] However, using different CTV–PTV margins for these landmarks (such as C1-C5, mandible and sphenoid sinus) was complicated to implement in clinical practice. In our study, the CTV/OAR expanding margin was calculated without considering the rotation error or the local deformation. It should be kept in mind that rotation error correction is highly important and significantly influences the dose distribution.[20] However, few radiotherapy departments currently use clinical corrections for rotation errors. Thus, the proper CBCT registration strategy is particularly important in clinical use. Based on these results, special care should be paid

Table 3. ROC analysis using the $PTV_{ROI}$ registration results with a threshold of 2 mm to classify the need of couch shift for different ROIs (online correction threshold)

| Directions | | ROIs | | | | | | | | | |
|---|---|---|---|---|---|---|---|---|---|---|---|
| | | C1 | C2 | C3 | C4 | C5 | C6 | C7 | S | M | L |
| ML | AUC | 0.58 | 0.57 | 0.56 | 0.56 | 0.55 | 0.53 | 0.51 | 0.55 | 0.55 | 0.54 |
| | SE | 0.07 | 0.07 | 0.07 | 0.07 | 0.07 | 0.06 | 0.06 | 0.07 | 0.07 | 0.06 |
| | $p_{value}$ | 0.11 | 0.16 | 0.22 | 0.23 | 0.3 | 0.56 | 0.81 | 0.26 | 0.27 | 0.43 |
| | L limit | 0.44 | 0.43 | 0.43 | 0.43 | 0.42 | 0.4 | 0.39 | 0.42 | 0.42 | 0.42 |
| | U limit | 0.71 | 0.7 | 0.69 | 0.69 | 0.68 | 0.65 | 0.63 | 0.69 | 0.69 | 0.66 |
| SI | AUC | 0.63 | 0.61 | 0.63 | 0.64 | 0.63 | 0.64 | 0.64 | 0.61 | 0.66 | 0.64 |
| | SE | 0.06 | 0.06 | 0.05 | 0.05 | 0.06 | 0.06 | 0.06 | 0.06 | 0.05 | 0.04 |
| | $P_{value}$ | 0.00 | 0.01 | 0.00 | 0.00 | 0.00 | 0.00 | 0.00 | 0.01 | 0.00 | 0.00 |
| | L limit | 0.52 | 0.5 | 0.52 | 0.53 | 0.52 | 0.53 | 0.53 | 0.5 | 0.56 | 0.56 |
| | U limit | 0.73 | 0.72 | 0.74 | 0.75 | 0.74 | 0.75 | 0.74 | 0.72 | 0.76 | 0.73 |
| AP | AUC | 0.77 | 0.76 | 0.73 | 0.65 | 0.59 | 0.58 | 0.59 | 0.79 | 0.79 | 0.52 |
| | SE | 0.05 | 0.05 | 0.05 | 0.05 | 0.06 | 0.06 | 0.05 | 0.04 | 0.05 | 0.05 |
| | $p_{value}$ | 0.00 | 0.00 | 0.00 | 0.00 | 0.09 | 0.10 | 0.07 | 0.00 | 0.00 | 0.76 |
| | L limit | 0.68 | 0.67 | 0.63 | 0.56 | 0.47 | 0.47 | 0.49 | 0.71 | 0.69 | 0.42 |
| | U limit | 0.87 | 0.85 | 0.82 | 0.75 | 0.7 | 0.69 | 0.7 | 0.88 | 0.88 | 0.62 |

AP, antero posterior; AUC, area under the curve; ML, mediolateral; PTV,planning target volume; ROI, region of interest; SE, standard error; SI, superior–inferior.

AUC, Area under curve (low accuracy: the AUC value range 0.5 to 0.7; high accuracy: the AUC value > 0.9 ). SE, standard error; medium accuracy: the AUC value range 0.7 to 0.9; $p_{value}$ less than 0.05 indicate that the ROI had discrimination power to classify the need for couch shift according to 2 mm online correction threshold of $PTV_{ROI}$. L limit, the lower limit of 95% confidence limits, U limit, the upper limit of 95% confidence limits.

to the patients with a 5-mm uniform margin in NPC radiotherapy even with the use of image guidance.

In our study, the set-up error in the AP direction was obvious, and this was exactly the direction in which the $S_{ROI}$ and the brain stem were anatomically connected. The blurring effect of random errors leads to small decrease in dose at the edges of the high-dose regions that will moderately affect all patients. In contrast, systematic errors lead to shifts in the dose, which would strongly affect some patients.[6] Thus, when $S_{ROI}$ is involved in the registration, we should pay particular attention to the systematic local set-up error in the AP direction. When consecutive local set-up errors of substructures (*i.e.* generated from the first 3–5 treatment fractions) of 2°/2 mm are identified by the sphenoid sinus region, re-planning is recommended to compensate for these deformation errors.[15,18,21] To guarantee a safe treatment, we recommend that the typical isodose line of the planned dose distribution should be overlapped with the registration images and used as an important reference line for the determination of couch correction.

Large local set-up errors primarily occurred in the lower neck.[1,19] Typical examples are the larynx and hyoid regions, which exhibit relatively large movements in the SI direction. An OAR-PRV margin of 5 mm is not sufficient in these cases.[9] Furthermore, the position of the thyroid is associated with the movement of the larynx. Pre-treatment evaluation of the thyroid dose ($V_{45}$, the dose restraint for the thyroid) is an effective method for avoiding hypothyroidism.[22] In the region of the lower neck, great margins are needed if either of these systems is used to treat caudal target volumes in proximity to the shoulder level.[23] Thus, a margin wider than 5 mm for the spinal cord is feasible. For patients with the metastatic lymph node ($GTV_{nd}$) located in the lower neck, the CTV–PTV margin should be 8 mm to ensure a sufficient dose irradiation due to the large deformation error. The local deformation error is not the only factor that affects the delivery dose. Individual tumour shrinkage and shape changes in the body and parotid also account for set-up errors. To observe these changes, weekly CBCT scans are essential in clinical practice following the offset of the system error based on the first three to five fractions.[19] More effective personalised immobilisation is required for lower neck radiotherapy.

## CONCLUSION

In radiotherapy for NPC patients who are immobilised with the standard headrest and thermoplastic mask, only the local set-up errors of $C1_{ROI}$-$C4_{ROI}$, $M_{ROI}$, and $S_{ROI}$ can be represented using PTV as a reference ROI with a 5 mm margin for CBCT registration. Using these ROIs as an integral reference, ROI was better than individual bony landmark.

## FUNDING

This research is supported by the Science and Technology Support Program of Sichuan province, China (No.2016FZ0086) in the study design.

## REFERENCES


1. van Kranen S, van Beek S, Rasch C, van Herk M, Sonke JJ. Setup uncertainties of anatomical sub-regions in head-and-neck cancer patients after offline CBCT guidance. *Int J Radiat Oncol Biol Phys* 2009; **73**: 1566–73. doi: https://doi.org/10.1016/j.ijrobp.2008.11.035
2. Giske K, Stoiber EM, Schwarz M, Stoll A, Muenter MW, Timke C, et al. Local setup errors in image-guided radiotherapy for head and neck cancer patients immobilized with a custom-made device. *Int J Radiat Oncol Biol Phys* 2011; **80**: 582–9. doi: https://doi.org/10.1016/j.ijrobp.2010.07.1980
3. van Beek S, van Kranen S, Mencarelli A, Remeijer P, Rasch C, van Herk M, et al. First clinical experience with a multiple region of interest registration and correction method in radiotherapy of head-and-neck cancer patients. *Radiother Oncol* 2010; **94**: 213–7. doi: https://doi.org/10.1016/j.radonc.2009.12.017
4. Kapanen M, Laaksomaa M, Tulijoki T, Peltola S, Wigren T, Hyödynmaa S, et al. Estimation of adequate setup margins and threshold for position errors requiring immediate attention in head and neck cancer radiotherapy based on 2D image guidance. *Radiat Oncol* 2013; **8**: 212. doi: https://doi.org/10.1186/1748-717X-8-212
5. Graff P, Kirby N, Weinberg V, Chen J, Yom SS, Lambert L, et al. The residual setup errors of different IGRT alignment procedures for head and neck IMRT and the resulting dosimetric impact. *Int J Radiat Oncol Biol Phys* 2013; **86**: 170–6. doi: https://doi.org/10.1016/j.ijrobp.2012.10.040
6. BIR Working Party. *Geometric uncertainties in radiotherapy: Defining the planning target volume*. London: The British Institute of Radiology; 2003.
7. Bland JM, Altman DG. Comparing methods of measurement: why plotting difference against standard method is misleading. *Lancet* 1995; **346**: 1085–7.
8. Alemayehu D, Zou KH. Applications of ROC analysis in medical research: recent developments and future directions. *Acad Radiol* 2012; **19**: 1457–64. doi: https://doi.org/10.1016/j.acra.2012.09.006
9. Den RB, Doemer A, Kubicek G, Bednarz G, Galvin JM, Keane WM, et al. Daily image guidance with cone-beam computed tomography for head-and-neck cancer intensity-modulated radiotherapy: a prospective study. *Int J Radiat Oncol Biol Phys* 2010; **76**: 1353–9. doi: https://doi.org/10.1016/j.ijrobp.2009.03.059
10. Velec M, Waldron JN, O'Sullivan B, Bayley A, Cummings B, Kim JJ, et al. Cone-beam CT assessment of interfraction and intrafraction setup error of two head-and-neck cancer thermoplastic masks. *Int J Radiat Oncol Biol Phys* 2010; **76**: 949–55. doi: https://doi.org/10.1016/j.ijrobp.2009.07.004
11. Qi XS, Hu AY, Lee SP, Lee P, DeMarco J, Li XA, et al. Assessment of interfraction patient setup for head-and-neck cancer intensity modulated radiation therapy using multiple computed tomography-based image guidance. *Int J Radiat Oncol Biol Phys* 2013; **86**: 432–9. doi: https://doi.org/10.1016/j.ijrobp.2013.01.022
12. Dionisi F, Palazzi MF, Bracco F, Brambilla MG, Carbonini C, Asnaghi DD, et al. Set-up errors and planning target volume margins in head and neck cancer radiotherapy: a clinical study of image guidance with on-line cone-beam computed tomography. *Int J Clin Oncol* 2013; **18**: 418–27. doi: https://doi.org/10.1007/s10147-012-0395-7
13. Mongioj V, Orlandi E, Palazzi M, Deponti E, Marzia F, Stucchi C, et al. Set-up errors analyses in IMRT treatments for nasopharyngeal carcinoma to evaluate time trends, PTV and PRV margins. *Acta Oncol* 2011; **50**: 61–71. doi: https://doi.org/10.3109/0284186X.2010.509108
14. Chen AM, Farwell DG, Luu Q, Donald PJ, Perks J, Purdy JA. Evaluation of the planning target volume in the treatment of head and neck cancer with intensity-modulated radiotherapy: what is the appropriate expansion margin in the setting of daily image guidance? *Int J Radiat Oncol Biol Phys* 2011; **81**: 943–9. doi: https://doi.org/10.1016/j.ijrobp.2010.07.017
15. Zumsteg Z, DeMarco J, Lee SP, Steinberg ML, Lin CS, McBride W, et al. Image guidance during head-and-neck cancer radiation therapy: analysis of alignment trends with in-room cone-beam computed tomography scans. *Int J Radiat Oncol Biol Phys* 2012; **83**: 712–9. doi: https://doi.org/10.1016/j.ijrobp.2011.08.001
16. Duma MN, Kampfer S, Schuster T, Aswathanarayana N, Fromm LS, Molls M, et al. Do we need daily image-guided radiotherapy by megavoltage computed tomography in head and neck helical tomotherapy? The actual delivered dose to the spinal cord. *Int J Radiat Oncol Biol Phys* 2012; **84**: 283–8. doi: https://doi.org/10.1016/j.ijrobp.2011.10.073
17. Stoiber EM, Schwarz M, Huber PE, Debus J, Bendl R, Giske K. Comparison of two IGRT correction strategies in postoperative head-and-neck IMRT patients. *Acta Oncol* 2013; **52**: 183–6. doi: https://doi.org/10.3109/0284186X.2012.691210
18. Stoll M, Giske K, Debus J, Bendl R, Stoiber EM. The frequency of re-planning and its variability dependent on the modification of the re-planning criteria and IGRT correction strategy in head and neck IMRT. *Radiat Oncol* 2014; **9**: 175. doi: https://doi.org/10.1186/1748-717X-9-175
19. Djordjevic M, Sjöholm E, Tullgren O, Sorcini B. Assessment of residual setup errors for anatomical sub-structures in image-guided head-and-neck cancer radiotherapy. *Acta Oncol* 2014; **53**: 646–53. doi: https://doi.org/10.3109/0284186X.2013.862593
20. Fu W, Yang Y, Yue NJ, Heron DE, Saiful Huq M. Dosimetric influences of rotational setup errors on head and neck carcinoma intensity-modulated radiation therapy treatments. *Med Dosim* 2013; **38**: 125–32. doi: https://doi.org/10.1016/j.meddos.2012.09.003
21. Pang PP, Hendry J, Cheah SL, Soong YL, Fong KW, Wee TS, et al. An assessment of the magnitude of intra-fraction movement of head-and-neck IMRT cases and its implication on the action-level of the imaging protocol. *Radiother Oncol* 2014; **112**: 437–41. doi: https://doi.org/10.1016/j.radonc.2014.09.008
22. Kim MY, Yu T, Wu HG. Dose-volumetric parameters for predicting hypothyroidism after radiotherapy for head and neck cancer. *Jpn J Clin Oncol* 2014; **44**: 331–7. doi: https://doi.org/10.1093/jjco/hyt235
23. Rotondo RL, Sultanem K, Lavoie I, Skelly J, Raymond L. Comparison of repositioning accuracy of two commercially available immobilization systems for treatment of head-and-neck tumors using simulation computed tomography imaging. *Int J Radiat Oncol Biol Phys* 2008; **70**: 1389–96. doi: https://doi.org/10.1016/j.ijrobp.2007.08.035